4. S. Tan, R. Boyle, J. Whiteside, and R. Anderson, "Nonlinear stress–strain relation for metal meshes," Raket. Tekh. Kosmonavtika, No. 6 (1980).
5. L. P. Vishnyakov and L. I. Feodos'eva "Nonlinear deformation of metal knit with rhombic structural elements," in: Problems of the Strength of Elements of Devices [in Russian], MIP, Moscow (1990).
6. B. A. Dryuyanov, Applied Theory of the Plasticity of Porous Media [in Russian], Mashinostroenie, Moscow (1989).
7. R. Hill, "General method of metal-working analysis," in: Mechanics. Collected Translations of Foreign Literature [in Russian], No. 3 (1964).
8. V. V. Skorokhod, Rheological Foundations of Sintering Theory [in Russian], Naukova Dumka, Kiev (1972).
9. B. I. Geresnev, K. I. Ezerskii, and E. V. Trushin, Physical Foundations and Practical Applications of Hydrostatic Extrusion [in Russian], Nauka, Moscow (1981).

CALCULATION OF THE RESIDUAL STRESSES IN WELDED JOINTS OF HARD ALLOYS WITH STEELS BY THE BOUNDARY ELEMENTS METHOD

V. N. Milenin, I. A. Filimonenko, and L. I. Shkutin

UDC 539.3

We have used the boundary elements method to study the pattern of the residual-stress distribution in welded cylindrical specimens of a hard alloy and steel. The experimentally observed expansion of steel as a result of internal transformations is prescribed by uniform bulk deformation. It has been proved theoretically and experimentally that the concentration of the axial tensile stresses on the cylindrical surface in the zone of the welded joint causes the hard alloy to fracture. It has also been proved that controlling the cooling rate not only reduces the residual stresses and prevents fracturing of the hard alloy but also forms a residual capable of compensating, to a degree, for the working stresses in the welded member.

Mechanism of Residual-Stress Formation. Hard alloys are used in industry to fit out boring, cutting, stamping, and other tools. Permanent connections are made by welding, brazing, anf gluing. Welded joints are strongest. The existence of residual stresses as an inevitable consequence the thermal conditions of the welding, however, weakens the welded joint and may cause the hard alloy to fracture.

The mechanism of stress formation in welded joints is associated with the cooling process and is due to the difference in the thermal expansion coefficients of the materials being welded. Reduction of the residual stresses is promised by using various compensating metal spacers and powder interlayers and by artificially producing porosity in the zone of the joint [1]. As this analysis shows, it is more promising to control the stressed state by means of the volume expansion effect that accompanies the structural transformations of the steel during cooling.

The main laws of stress formation during welding of diverse materials can be traced on the simplest model of uniaxial strain. During cooling in the free state the thermal strains of the steel and the hard alloy are $\alpha_1\Delta T$ and $\alpha_2\Delta T$, respectively (ΔT is the temperature drop and α_1 and α_2 are the thermal expansion coefficients (TECs) of the steel and the alloy). If ε_0 is the structural deformation of the steel and ε_1 and ε_2 are the residual strains of the steel and the alloy, then the condition for a rigid joint is

$$\varepsilon_2 + \alpha_2\Delta T = \varepsilon_0 + \varepsilon_1 + \alpha_1\Delta T.$$

From this we determine the residual strain of the hard alloy

$$\varepsilon_2 = \varepsilon_1 + \varepsilon_0 - (\alpha_2 - \alpha_1)\Delta T.$$

Krasnoyarsk. Translated from Prikladnaya Mekhanika i Tekhnicheskaya Fizika, No. 1, pp. 150-154, January-February, 1993. Original article submitted December 16, 1991.

 0021-8944/93/3401-0144$12.50

TABLE 1

Material	TEC, 10^{-6} K^{-1}	Poisson's ratio	Young's modulus, GPa	Elastic limit, GPa	Ultimate strength, GPa	
					tension	compression
Steel	11,6	0,30	200	0,36	0,61	—
Alloy	5,1	0,27	700	1,50	0,80	4

As we see, it depends on the structural strain of the steel and the jump in the free thermal strain. No residual strains (and stresses) exist in the steel and the alloy when $\varepsilon_0 = (\alpha_2 - \alpha_1)\Delta T$: the structural strain cancels the thermal jump. Since $\Delta T < 0$ and $\alpha_1 > \alpha_2 > 0$, the compensating value of the structural strain is positive (expansion).

This simple analysis confirms that the residual stresses in a hard alloy by the strain is due to volume expansion of the steel during its structural transformation as it is cooled.

For real welded members this scheme is expressed as a complex kinetic-thermodynamic problem. In this article we represent it as a linear problem of thermoelasticity. The objects studied were cylindrical bimetallic specimens of steel and hard alloy. The characteristics of the materials welded are shown in Table 1.

A numerical analysis of the elastic thermal stresses in composite axisymmetric bodies of finite dimensions was made in [2, 3]. An algorithm of the variational-difference method was proposed in [2] for the calculation of cylindrical specimens of steel and hard alloy, but the subject of control of residual stresses was not raised. In [3] two-layered disks were analyzed by the method of finite elements. Prestressing one of the layers substantially reduced the residual stresses.

In this study the problem of the formation and control of residual thermal stresses in welded cylindrical specimens is solved by the method of boundary elements, which evidently is best suited to the specifics of the problem. The theoretical results are checked experimentally.

Mathematical Formulation and Numerical Analysis of the Problem. In the cylindrical coordinate system we consider a piecewise-homogeneous body in the shape of a round cylinder of radius R. The plane $z = 0$ divides it into two parts of different materials with heights Z_1 and Z_2. It is assumed that the material of each cylindrical part is homogeneous and isotropic, the two parts are rigidly joined, their temperatures does not depend on the coordinates, and the thermal expansion coefficients α_1 and α_2 are temperature-independent.

The deformation of a piecewise-homogeneous cylinder during cooling from T_0 to T is studied within the framework of the linear axisymmetric problem of thermoelasticity. The displacement vector is determined by two components, radial u and axial v, the strain tensor by four components,

$$\varepsilon_1 = \partial u/\partial r,\ \varepsilon_2 = \partial v/\partial z,\ \varepsilon_3 = u/r,\ \varepsilon_4 = \partial v/\partial r + \partial u/\partial z,$$

and the stress tensor by four components,

$$\sigma_n = 2G(\gamma_n + (1 - 2\nu)^{-1}\nu\gamma),\ \sigma_4 = G\gamma_4.$$

Here $\gamma_n = \varepsilon_n - \varepsilon_0 + \alpha(T_0 - T)$; $\gamma_4 = \varepsilon_4$; $\gamma = \gamma_1 + \gamma_2 + \gamma_3$ is the shear modulus; ν is Poisson's ratio; and $3\varepsilon_0$ is the structural strain due to volume expansion and the row index assumes the values 1, 2, and 3.

The axisymmetric problem of thermoelasticity was solved by direct methods of boundary elements [4]. The boundary of the region was divided into rectilinear elements with a regular condensation of the grid near the sharp corners. The given and unknown boundary functions were assumed to be constant on an element. The integrals were calculated from the Gauss formula with division of the boundary element into subelements in the neighborhood of a singular point.

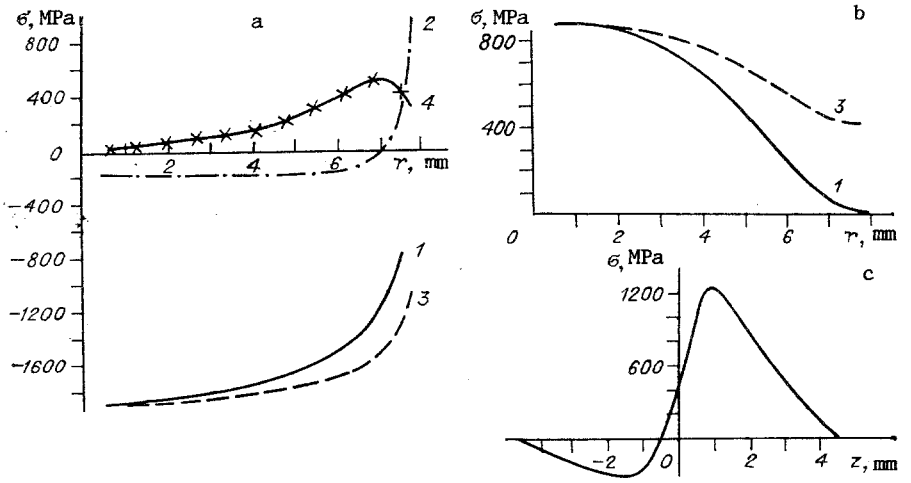

Fig. 1

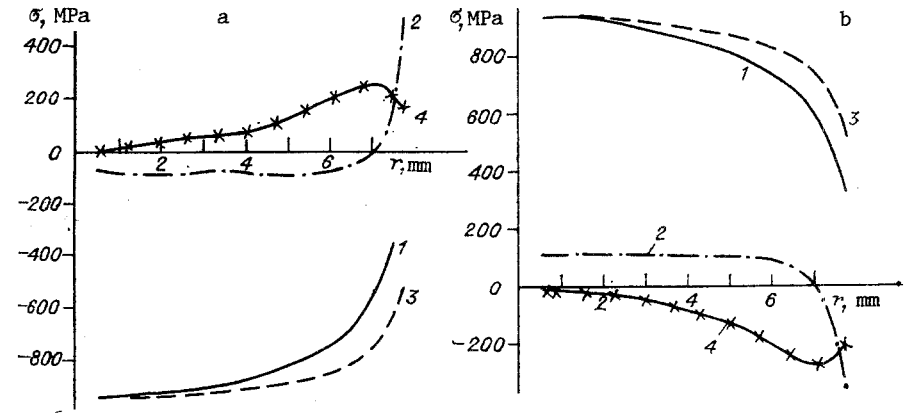

Fig. 2

The proposed formulation of the problem and its numerical analysis by the method of boundary elements made it possible to study the distribution of the residual stresses in cooled welded specimens of steel and hard alloy, depending on the structural strains of the steel. The results of the numerical analysis are shown in Figs. 1 and 2. All the data were obtained at a temperature drop of $T_0 - T = 100$ K. Lines 1-4 are the graphs of the radial (σ_{rr}), axial (σ_{zz}), circumferential ($\sigma_{\phi\phi}$), and shear ($\sigma_{zr} = \sigma_{rz}$) stresses, respectively.

Figure 1 illustrates the stress distribution in a welded specimen of steel and hard alloy with dimensions R = 8 mm, $Z_2 = Z_1 = 5$ mm when cooled by 100 K without allowance for the structural strain of the steel; a is the stress distribution in the hard alloy along the radius of the contact section z = 0. The radial and circumferential stresses are compressive and decrease monotonically in absolute value in the direction from the axis to the cylindrical surface. Their values on the axis coincide with each other. The axial stresses, being compressive and low inside the cylinder, become tensile and high on the surface. The shear stress increases from the center to the periphery, but is zero on the surface itself and so it drops abruptly at the cylindrical surface.

Figure 1b demonstrates the distribution of the radial and circumferential stresses on the free end surface $z = Z_2$ of the hard alloy. Being tensile, they decrease from the center to the periphery, but their values at the center are worthy of attention. There are no axial shear stresses on that surface. Figure 1c shows the distribution of the axial stresses over the cylindrical surface r = R of the specimen. As we see, the axial tensile stresses in the alloy reach maximum near and not at the point of contact with the steel (z = 0). In the neighborhood of this point the steel also undergoes considerable tensile stresses.

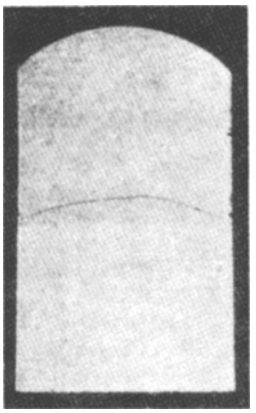

Fig. 3

The effect of the structural strain of the steel on the stressed state of the welded specimen is shown in Fig. 2. The structural strain ε_0 is given in fractions of the jump $(\alpha_2 - \alpha_1)\Delta T$ in the free thermal strain. Besides the value $\varepsilon_0 = (\alpha_2 - \alpha_1)\Delta T$, to which nearly zero stresses correspond, we consider two values of ε_0 namely 50 and 150% of the jump, to which the calculated data given in Fig. 2 correspond. Its graphs have the same sense as in Fig. 1a. A 50% structural strain of the steel decreases the residual stresses in the hard alloy by half (Fig. 2a) in comparison with the data of Fig. 1a. At a 150% strain the stressed state is inverted: the tensile stresses become compressive and the compressive stresses become tensile (Fig. 2b).

Experimental Analysis of Residual Stresses. The values of the structural strains of the steel considered in the calculations were ensured in the experiment by using appropriate cooling. The temperature drops were 700-800 K. The cooling rates were chosen on the basis of an analysis of the anisothermal diagram of austenitic decomposition and ranged from 5 to 120 K/sec, encompassing the entire region of structural transformations in the steel. We studied the structure and phase state with generally accepted methods of metallographic analysis. The residual stresses were determined by x-ray methods on the end plane of the hard alloy. The experiments determined that at cooling rates of 5-10 K/sec the decomposition of austenite is accompanied by the formation of pearlite-sorbite structures. The structural strains in the steel in this form of transformations are insufficient to compensate for the thermal stresses due to the difference of the thermal expansion coefficients of the materials being welded. Tensile stresses of 300-400 MPa arise on the end plane of the hard alloy. Bainite-martensite structures are formed in the range of cooling rates from 70 to 80 K/sec. The measured values of the stresses varied from −50 to 80 MPa. Martensite structures predominated in the steel when the cooling rate increased to 100 K/sec or higher. The stresses measured on the surface of the alloy were compressive in this case. Their values lay in the range 100-150 MPa. The change of sign by the stresses shows that the structural strains exceed the thermal strains.

Comparison of the calculated and experimental results shows them to be in qualitative agreement. The quantitative difference is due to several factors: the possible nonuniformity of the structures in the cross sections of the specimen because of the different hardenabilities of the surface and central portions of the steel cylinder; the plastic strains of the steel; and the stress relaxation. In actual fact, the calculations show that at a given temperature drop the stresses in the steel exceed the elastic limit and, therefore, plastic zones inevitably appear. The pores and defects in the structure of the hard alloy are conducive to stress relaxation.

When the thermal stresses in the hard alloy approach the ultimate strength the development of microcracks leads to fracture. A typical picture of the fracture of a hard alloy after welding to steel at low cooling rates is shown in Fig. 3. Microcrack nucleation and fracture of the alloy begin on the cylindrical surface in the zone of the welded joint with the steel. According to calculation, that is where the axial tensile stresses are concentrated. Further development of the fracture is also promoted by shear stresses concentrated at the cylindrical surface of the specimen. The radial and circumferential stresses, being compressive in the zone of the joint, cannot be responsible for the fracture of the hard

alloy since its compressive strength is incomparably higher than its tensile strength. For this reason since it provides no information about the stresses, the stress intensity cannot be a strength criterion for the hard alloy. The calculations and experiments demonstrate that the axial tensile stresses on the cylindrical surface in the zone of the welded joint is such a criterion.

LITERATURE CITED

1. N. A. Klochko, Fundamentals of the Technology of Brazing and Heat Treatment of a Hard-Alloy Tool [in Russian], Metallurgiya, Moscow (1981).
2. T. G. Beleicheva and K. K. Ziling, "Thermoelastic axisymmetric problem for a two-layer cylinder," Prikl. Mekh. Tekh. Fiz., No. 1 (1978).
3. A. S. Tsybenko, A. L. Maistrenko, V. N. Kulakovskii, et al., "Analysis of the technological stress in two-layer SiC—Si disks," Probl. Prochn., No. 11 (1982).
4. C. A. Brebbia, J. Telles, and L. Browbell, Boundary Elements, Springer-Verlag (1984).

EFFECT OF ELECTRON TRANSFER ON THE COLD RESISTANCE OF THE NEAR-SEAM ZONE IN ELECTRIC ARC WELDING

Ya. S. Semenov, M. N. Sivtsev, and A. A. Argunova

UDC 539.2:539.172.3:621.78

Electron transfer can be used to produce atomic fluxes and concentration shifts in alloys and, hence, to study the mobility and diffusion coefficients of atoms [1, 2]. It is also interesting technologically. Electron transfer has been shown to be responsible for damage in metal strips in integrated circuits. On the other hand, it has been used successfully to remove interstitial impurities from metals [3]. Accordingly, we developed [4] a procedure for treating the near-seam zone (NSZ) by the current of the electric welding arc, which lowered the cold brittleness temperature but did not determine why this happened.

In this work we study the microstructure of the near-seam zone and use Mössbauer spectroscopy to study the electron transfer parameters. The following procedure has been developed for Mössbauer studies of electron transfer. A dc current, regulated with an external variable resistance R, is passed through a specimen absorber. The electric current and the voltage applied are determined by instruments built into the power supply.

When a high electric current flows through it the specimen is heated by Joule heating, which cannot be disregarded when determining the electron transfer. In this case the absorber must be placed in a cryostat to keep the specimen at a constant temperature.

Using the scheme described above, we studied the electron-transfer parameters of steels St.3 and 14Cr2MgMoB. These steels are used extensively in the national economy of northeast Russia and lend themselves well to welding. Steel St.3 is customarily used in GOST (All-Union State Standard) welding tests. They can thus serve as a standard experimental material.

Foils for the specimens were prepared by the generally accepted method. Wires to carry the current were welded to the specimen. Mössbauer spectra were obtained on an electrodynamic spectrometer with a Co^{57} γ-ray source.

Figure 1 shows the resonance spectra of St.3 and 14Cr2MgMoB steels with a different current (horizontal axis shows the channel numbers and the vertical axis, the relative intensities: a) shows the Mössbauer spectra of St.3 steel in the initial state and during passage of a current of density 70 mA/mm^2). The resonance spectrum of St. 3 steel in the initial state consists of the sum of the separable partial spectra of ferrite and martensite. With the passage of electronic current the resonance lines become narrower and the martensite spectrum is virtually inseparable. The resonance spectra of 14Cr2MgMoB steel are shown

Yakutsk. Translated from Prikladnaya Mekhanika i Tekhnicheskaya Fizika, No. 1, pp. 154-160, January-February, 1993. Original article submitted October 17, 1991; revision submitted January 8, 1992.

0021-8944/93/3401-0148$12.50